Measuring the system size dependence of the strangeness production with ALICE

Roman Nepeivoda[1,*] for the ALICE Collaboration

[1]Lund University Department of Physics, Division of Particle and Nuclear Physics, Lund, Sweden

Abstract. The system size dependence of strangeness production in high-energy collisions was studied using Run 2 data from the ALICE experiment at the LHC. The analysis examines the ratios of strange hadron yields to pion yields as a function of mid-rapidity charged particle multiplicity $\langle \mathrm{d}N_{\mathrm{ch}}/\mathrm{d}\eta \rangle_{|\eta|<0.5}$, offering insights into the mechanisms driving strangeness enhancement across different collision systems (pp, p–Pb and Pb–Pb). The yield ratios exhibit a continuous rising trend from low-multiplicity pp collisions at $\sqrt{s}$ = 7 TeV to central Pb–Pb collisions at $\sqrt{s_{\mathrm{NN}}}$ = 5.02 TeV. Additionally, the evolution of the mean transverse momentum ($\langle p_{\mathrm{T}} \rangle$) for various strange hadrons ($\mathrm{K^0_S}$, Λ ($\bar{\Lambda}$), $\Omega^{\pm}$, $\Xi^{\pm}$) is analyzed, revealing that $\langle p_{\mathrm{T}} \rangle$ does not connect smoothly between different collision systems, with harder spectra observed in high-multiplicity pp collisions compared to the peripheral Pb–Pb collisions. Finally, performance plots from LHC Run 3 are presented, showcasing the purity of Ξ^- and Ω^- invariant mass distributions and highlighting the enhanced detector capabilities in Run 3.

1 Introduction

Studying strangeness production in high-energy collisions is crucial for understanding the underlying dynamics of the quark-gluon plasma (QGP) and the hadronization process in quantum chromodynamics (QCD). Strangeness, a quantum number carried by strange quarks, is particularly sensitive to the conditions created in these collisions. Strangeness production has been widely studied across various systems and energies, from proton-proton (pp) [1, 2] and proton-lead (p–Pb) [3, 4] to lead-lead (Pb–Pb) [5, 6] collisions in the ALICE experiment at the Large Hadron Collider (LHC), providing key insights into the collective behavior of particles and the mechanisms driving hadronization.

The design of the ALICE experiment, optimized for the study of QGP in heavy-ion collisions, also allows for precise measurements in smaller systems, making it possible to compare the behavior of strange hadrons across different collision environments [7]. This comparative analysis is essential for probing the onset of collective effects and understanding the evolution of the QGP.

In heavy-ion collisions, where a QGP is expected to form, strangeness enhancement – defined as an increase in the production of strange hadrons relative to non-strange hadrons – has been considered a signature of QGP formation. However, recent observations in smaller systems, such as pp [1, 2] and p–Pb [3, 4] collisions, have challenged this traditional view.

*e-mail: roman.nepeivoda@cern.ch

These findings suggest that strangeness enhancement may not be exclusive to heavy-ion collisions. Rather, mechanisms other than QGP formation – such as increased parton density or the presence of strong color fields – could also play a significant role in driving strangeness enhancement in smaller collision systems, calling for a deeper understanding of the underlying physics.

2 ALICE detector

The ALICE detector is specifically designed to study the properties of the QGP formed in heavy-ion collisions. It comprises several subsystems used for tracking, vertexing, and particle identification. The Time Projection Chamber (TPC) [8] serves as the primary tracking device, offering excellent spatial resolution and particle identification capabilities through specific ionization energy loss ($\mathrm{d}E/\mathrm{d}x$) measurements. The Inner Tracking System (ITS) [9] provides precise vertex reconstruction and complements the TPC in tracking low-momentum particles. The Time-of-Flight (TOF) [10] detector further aids in particle identification by measuring the flight time of particles with high precision.

3 Strangeness scaling with charged-particle multiplicity

One of the key observables in the studies of strange hadron production is the ratio of p_{T}-integrated strange hadron yields to pion yields as a function of the charged-particle multiplicity at mid-rapidity ($\langle \mathrm{d}N_{\mathrm{ch}}/\mathrm{d}\eta \rangle_{|\eta|<0.5}$). As multiplicity increases, this ratio rises, particularly for hadrons with higher strangeness content, offering a direct comparison of strangeness production across different collision systems and energies.

Previous measurements have demonstrated that these ratios follow a smooth, continuous trend from low-multiplicity pp collisions to central Pb–Pb collisions [1–7]. The left panel of Fig. 1 shows the preliminary ALICE results for the ratios of integrated yields between strange hadrons and pions in Pb–Pb collisions at $\sqrt{s_{\mathrm{NN}}} = 5.02$ TeV (squares). These are compared with results from pp collisions at $\sqrt{s} = 7$ TeV [1] and $\sqrt{s} = 13$ TeV [2] (open and closed circles, respectively), p–Pb collisions at $\sqrt{s_{\mathrm{NN}}} = 5.02$ TeV [3] (diamonds), and Pb–Pb collisions at $\sqrt{s_{\mathrm{NN}}} = 2.76$ TeV [5, 6] (stars). The new data reconfirm this smooth scaling, suggesting that the increase in strange hadron production relative to pions is largely driven by the charged-particle multiplicity rather than being system- or energy-specific. Notably, a previously observed hint of a decreasing Ξ/π ratio observed in central Pb–Pb collisions at $\sqrt{s_{\mathrm{NN}}} = 2.76$ TeV is not supported by the new data at $\sqrt{s_{\mathrm{NN}}} = 5.02$ TeV, reinforcing the consistent scaling of strangeness production across different collision systems and energies.

Another critical observable is the mean transverse momentum ($\langle p_{\mathrm{T}} \rangle$) of strange hadrons, which provides insights into collective motion and kinetic freeze-out conditions. Interestingly, rather than showing a smooth connection across different collision systems, the evolution of $\langle p_{\mathrm{T}} \rangle$ with increasing multiplicity exhibits system-dependent behaviour, as seen in the right panel of Fig. 1. Harder spectra are observed in high-multiplicity pp collisions compared to peripheral Pb–Pb collisions. It is important to note that the $\langle p_{\mathrm{T}} \rangle$ data are gathered at the same center-of-mass energy of $\sqrt{s_{\mathrm{NN}}} = 5.02$ TeV for different collision systems, ensuring consistent comparisons. However, the same multiplicities across different systems do not necessarily reflect the same underlying particle production mechanisms. In high-multiplicity pp collisions, there is a bias toward events dominated by hard scatterings. This contrasts with peripheral Pb–Pb collisions where similar multiplicities could arise from several softer pp interactions. As discussed in [11], this difference can be explained using the core-corona formalism, where higher p_{T} values are associated with particles originating from the "core", a radially expanding medium, rather than from a "corona", which behaves as a decaying static droplet.

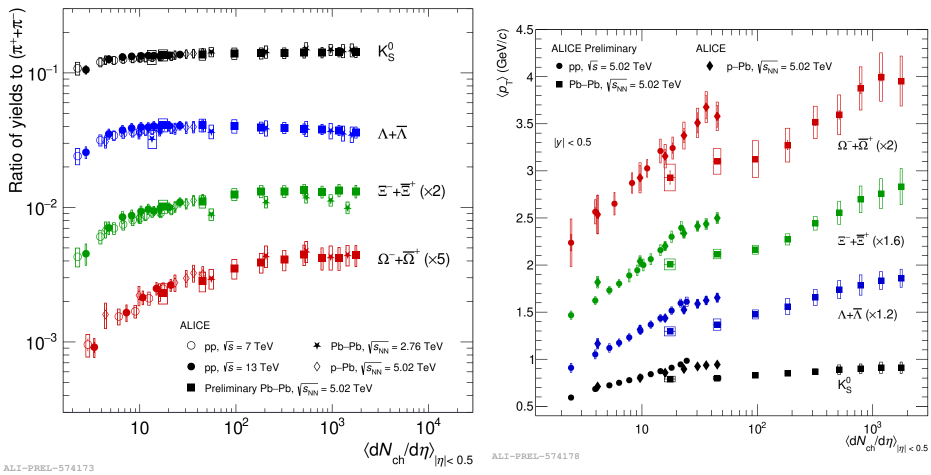

Figure 1. (left) The ratio of p_T-integrated K^0_S, Λ ($\bar{\Lambda}$), Ω, and Ξ strange particle yields to the corresponding pion yields as a function of $\langle dN_{ch}/d\eta\rangle_{|\eta|<0.5}$ in Pb–Pb collisions at $\sqrt{s_{NN}} = 2.76$ TeV [5, 6] (stars) and $\sqrt{s_{NN}} = 5.02$ TeV (squares) compared to pp collisions at $\sqrt{s} = 7$ TeV [1] and $\sqrt{s} = 13$ TeV [2] (open and closed circles, respectively), and p–Pb collisions at $\sqrt{s_{NN}} = 5.02$ TeV [3] (diamonds). (right) The average transverse momentum $\langle p_T\rangle$ dependence on the particle density in Pb–Pb collisions at $\sqrt{s_{NN}} = 5.02$ TeV (square markers). Results for pp and p–Pb [3, 4] collisions at the same center-of-mass energy are shown as dots and diamonds, respectively. Error bars indicate statistical uncertainties, while boxes represent total systematic uncertainties.

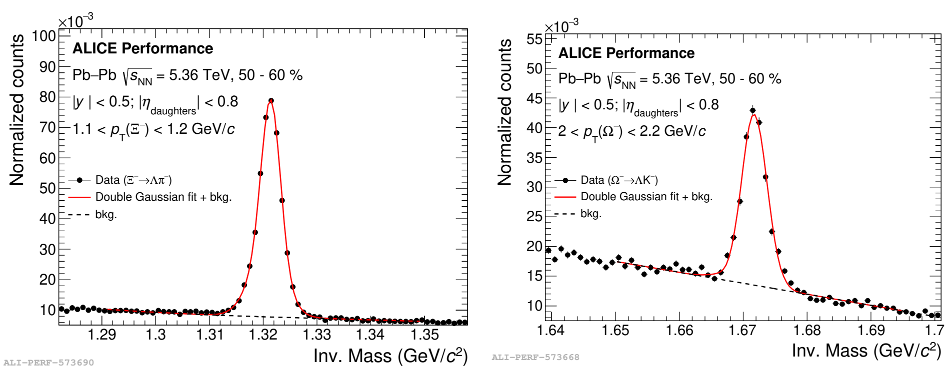

Figure 2. Invariant mass distributions of Ξ^- (left) and Ω^- (right) baryons measured in Pb–Pb collisions at $\sqrt{s_{NN}} = 5.36$ TeV in the 50–60% centrality class. The left panel shows the invariant mass distribution of $\Xi^- \rightarrow \Lambda\pi^-$ in $1.1 < p_T(\Xi^-) < 1.2$ GeV/c, while the right panel shows the invariant mass distribution of $\Omega^- \rightarrow \Lambda K^-$ in $2.0 < p_T(\Omega^-) < 2.2$ GeV/c. The data are fitted with a double Gaussian function for the signal plus a linear background component. The clear peaks around 1.322 GeV/c^2 and 1.672 GeV/c^2 correspond to the reconstructed masses of the Ξ^- and Ω^- baryons, respectively.

4 Performance of cascade reconstruction in Run 3

As ALICE transitioned into LHC Run 3, a substantial upgrade of its components has been undertaken, also allowing to enhance its performance in the reconstruction of strange particles. The new ITS2 [12] provides improved spatial resolution, while the TPC's GEM-based readout system ensures better handling of higher interaction rates [13]. These upgrades allow for data collection at higher rates with greater precision. This is evidenced by the ALICE minimum bias Pb–Pb dataset collected during Run 3, which is in one year of data taking already 40x larger than that from Run 2. The reconstructed invariant mass distributions of Ξ^- and Ω^- baryons, shown in Fig. 2, demonstrate the resolution and background suppression achieved with the upgraded detectors.

These advancements are not merely incremental; they mark a significant leap forward in the experiment's capability to probe the QGP and explore the properties of QCD in heavy-ion collisions. As Run 3 progresses, the enhanced precision in strange hadron measurements will pave the way for deeper insights into the behavior of matter under extreme conditions, contributing to a broader understanding of the strong interaction.

References

[1] ALICE Collaboration, S. Acharya et al., "Multiplicity dependence of light-flavor hadron production in pp collisions at $\sqrt{s} = 7$ TeV". Phys. Rev. C **99(2)**, 024906 (2019).

[2] ALICE Collaboration, S. Acharya et al., "Multiplicity dependence of (multi-)strange hadron production in proton-proton collisions at $\sqrt{s} = 13$ TeV". Eur. Phys. J. C **80**, 1-26 (2020).

[3] ALICE Collaboration, J. Adam et al., "Multi-strange baryon production in p–Pb collisions at $\sqrt{s_{\rm NN}} = 5.02$ TeV". Phys. Lett. B **758**, 389-401 (2016).

[4] ALICE Collaboration, B. Abelev et al., "Multiplicity dependence of pion, kaon, proton and Λ production in p–Pb collisions at $\sqrt{s_{\rm NN}} = 5.02$ TeV". Phys. Lett. B **728**, 25–38 (2014).

[5] ALICE Collaboration, B. Abelev et al., "Multi-strange baryon production at mid-rapidity in Pb–Pb collisions at $\sqrt{s_{\rm NN}} = 2.76$ TeV". Phys. Lett. B **728**, 216-227 (2014).

[6] ALICE Collaboration, B. Abelev et al., "K^0_S and Λ production in Pb–Pb collisions at $\sqrt{s_{\rm NN}} = 2.76$ TeV". Phys. Rev. Lett. **111**, 222301 (2013).

[7] ALICE Collaboration, J. Adam et al., "Enhanced production of multi-strange hadrons in high-multiplicity proton–proton collisions". Nat. Phys. **13**, 535-539 (2017).

[8] ALICE Collaboration, J.Alme et al., "The ALICE TPC, a large 3-dimensional tracking device with fast readout for ultra-high multiplicity events". Nucl. Instrum. Meth. A **622**, 316-367 (2010).

[9] G. Contin and ALICE Collaboration, "Performance of the present ALICE Inner Tracking System and studies for the upgrade". JINST **7**, C06007 (2012).

[10] A. Akindinov et al., "Performance of the ALICE Time-Of-Flight detector at the LHC". Eur. Phys. J. Plus **128**, 44 (2013).

[11] K. Werner, "Core-corona procedure and microcanonical hadronization to understand strangeness enhancement in proton-proton and heavy ion collisions in the EPOS4 framework". Phys. Rev. C **109(1)**, 014910 (2024).

[12] F. Reidt and ALICE Collaboration, "Upgrade of the ALICE ITS detector". Nucl. Instrum. Meth. A **1032**, 166632 (2022).

[13] ALICE Collaboration, J. Adolfsson et al., "The upgrade of the ALICE TPC with GEMs and continuous readout". JINST **16**, P03022 (2021).